American Society of
Agricultural and Biological Engineers

An ASABE Meeting Presentation

Paper Number: 061159

Sensor Fusion for Roll and Pitch Estimation Improvement of an Agricultural Sprayer Vehicle

Lav Ramchandra Khot

Graduate Student, Agricultural and Biosystems Engineering, Iowa State University, Ames, IA, 50011 lav@iastate.edu

Lie Tang

Assistant Professor, Agricultural and Biosystems Engineering, Iowa State University, Ames, IA, 50011 lietang@iastate.edu

Brain L Steward

Associate Professor, Agricultural and Biosystems Engineering, Iowa State University, Ames, IA, 50011 bsteward@iastate.edu

Shufeng Han

Engineering Scientist, John Deere, Ag Management Solutions, Urbandale, Iowa hanshufeng@johndeere.com

Written for presentation at the
2006 ASABE Annual International Meeting
Sponsored by ASABE
Portland Convention Center
Portland, Oregon
9 - 12 July 2006

Abstract. *Sensor fusion technique has been commonly used for improving the navigation of autonomous agricultural vehicles by means of combining complimentary sensors mounted on such vehicles for the position and attitude angle measurements. In this research, sensor fusion via an Extended Kalman Filter (EKF) was used to integrate the attitude angle estimates from the Digital Elevation Models (DEMs) and Terrain Compensation Module (TCM) sensor to improve the roll and pitch angle measurements of a self propelled sprayer. The fusion algorithm was also developed to improve the three-dimensional positioning of the sprayer, in particular the elevation measurements of a GPS receiver mounted on the sprayer. Vehicle attitude and field elevation were measured at two speeds, 5.6 km/h and 9.6 km/h, using a set of onboard sensors including a real-time kinematic-*

differential GPS receiver (RTK-DGPS), a TCM sensor and an Inertial Measurement Unit (IMU). A second order auto-regressive (AR) model was developed to model the TCM roll and GPS-based pitch errors. The derived error states were incorporated into the EKF algorithm and the measurement noise covariance was estimated from the AR model, which limited the fine tuning of noise covariance to the process noise covariance only.

The EKF estimations were compared with the IMU measurements to validate the performance of the developed fusion algorithm. For the slow speed test data, the mean and standard deviation of the errors of roll (Mean: -0.2244º, Std. Dev.:1.471º) and pitch (Mean: 0.0597º, Std. Dev.: 0.6621º) from the EKF estimates were reduced considerably compared to that of the errors of roll (Mean: 0.2157º, Std. Dev.: 2.4610º) and pitch (Mean: 0.0473º, Std. Dev.: 1.3230º) from DEM. Medium speed test data also showed considerable improvement in the attitude angles estimated using the developed EKF algorithm. The fusion algorithm for improving the elevation measurement of the GPS also showed promising results. Thus, the fusion algorithm was effective in improving attitude and the navigational accuracy of the self-propelled agricultural sprayer, which in turn will also facilitate the automatic control of the implements that interact with the soil surface on undulated topographic surfaces.

Keywords: DEM, Roll, Pitch, Auto-regressive model, EKF.

Introduction

Digital Elevation Models (DEMs) have been increasingly used to model the terrain surfaces for harboring the important physical information about the terrain field conditions. DEMs can be useful in determining the attributes of the terrain such as slope and aspect, drainage basins, watershed features of the terrain, peaks, pits and other landforms for hydrological modeling. GPS (Global Positioning System) is one of the several developing technologies which are being commonly used to collect topographic data and create DEMs/ topographic maps (Yao and Clark, 2000; Colvocoresses, 1993). Clark and Lee (1998) found that among the stop-and-go and kinematic data collection using GPS, the kinematic receiver is more viable for a rapid development of the topography maps with high elevation accuracy. The single frequency GPS receiver provides reasonably accurate DEMs with elevation error of 10 to 12 cm for 10 or more passes of the data with the elevation bias as a major source of error (Yao and Clark, 2000).

Westphalen et al. (2004) evaluated DEMs using two different methods (1) the elevation measurements only, (2) the combination of the elevation with vehicle attitude measurements. The elevation and vehicle attitude measurements were taken using a self-propelled agricultural sprayer equipped with four Real Time Kinematic-Differential GPS (RTK-DGPS) receivers and an inertial measurement unit (IMU). DEMs developed by combining the elevation with the vehicle attitude measurements had Root-Mean-Square-Error (RMSE) of 10 to 11 cm compared to the RMSE of 15 cm for DEMs developed by the elevation measurements alone.

DEMs developed using the vehicle based measurements have been used by previous researchers to improve the vehicle navigation by means of the vehicle attitude estimates from DEMs. Elevation accuracy of the DEMs along with the other terrain variables is an important factor in estimating the roll and pitch of the vehicle. The attitude (roll and pitch) estimation of the vehicle from the previously generated DEMs can be useful for the vehicle localization improvement if their elevation errors can be reduced. Terrain Compensation Module (TCM) sensor (Deere & Co., Moline, IL) corrects the vehicle position based on the measured and corrected roll angles when the vehicle is working under the side slope conditions. One of the major problems with TCM sensor measurements is the high frequency noise associated with the roll measurements. In this scenario, an Extended Kalman Filter (EKF) can be useful to improve the roll and pitch estimates of a vehicle by fusing the attitude estimates from DEMs, roll measurements of the TCM sensor and GPS-based pitch estimates. The fusion algorithm is expected to improve the roll and pitch estimates by reducing the high frequency noise associated with TCM sensor as well as the elevation error in the DEMs. Therefore, the objectives of the presented research work were

To develop and implement a sensor fusion technique to combine attitude estimates from the DEMs, TCM and GPS sensors to improve the attitude of the self-propelled sprayer.

To improve the elevation measurement accuracy of the GPS receiver mounted on the self-propelled sprayer using enhanced sprayer attitude.

Instrumentation and Procedure

Data was collected from the Kulver Farm field located west of Ames, IA using John Deere self-propelled sprayer (model 4710, Deere & Co., Moline, IL). The field had total area of 0.55 acre (120 ft wide and 200 ft long). An IMU (model VG600AA-201, Crossbow Technology Inc., San Jose, Cal.), an RTK-GPS receiver (StarFire RTK, Deere & Co., Moline, IL) and a TCM sensor were mounted on the sprayer. The TCM sensor was mounted on the front top of the sprayer along with the GPS receiver at a distance of 1.93 m from the center. Another RTK-GPS receiver

was mounted on the left side at 1.63 m from front side and 1.53 m from the center of the sprayer. The sprayer was operated at two speeds: 5.6 km/h, 9.6 km/h; and the data collection was done at a sampling frequency of 5 Hz. In order to avoid data clustering at just few angles and to obtain well distributed data across the entire field range, the field area was traversed (fig. 1) at various orientations (e.g. along the slope, perpendicular to the slope and at 45º to the slope) so that the vehicle would experience a range of attitude angles during the data acquisition.

Several potential sources of errors existed when estimating the sprayer attitude angles from the DEMs. First, it was found that, given the small field where the work was done, the sprayer sometimes left the region of the field for which there was valid measurement data support. Second, as the sprayer traveled over the field surface, it interacted with small scale variations, micro-topography, of the field surface which were probably not captured in the DEM. For example, a 10 cm difference in the micro-topography from one side of the sprayer to the other will result in at least a 3.9º roll angle. Third, the RTK-GPS had elevation measurement errors which were propagated into the DEMs. These errors would ultimately end up as errors in the attitude angle estimates from the DEMs.

When TCM measured roll angles were regressed onto the IMU measured roll angles, for the data collected at 5.6 km/h, the slope of the regression line was 0.81, the y-intercept was 0.14 and R^2 was equal to 0.86. For the 9.6 km/h data, the regression line slope was 0.70, the y-intercept was 0.58 and R^2 equal to 0.58. There was a clear increase in the error in the TCM data, although based on the conversation with Deere engineers, the TCM signal is not a pure roll angle signal but a preprocessed signal which improves the vehicle steering response. The TCM sensor does not provide the pitch angle of the vehicle, so the pitch angle of the sprayer was estimated from a single RTK-GPS receiver

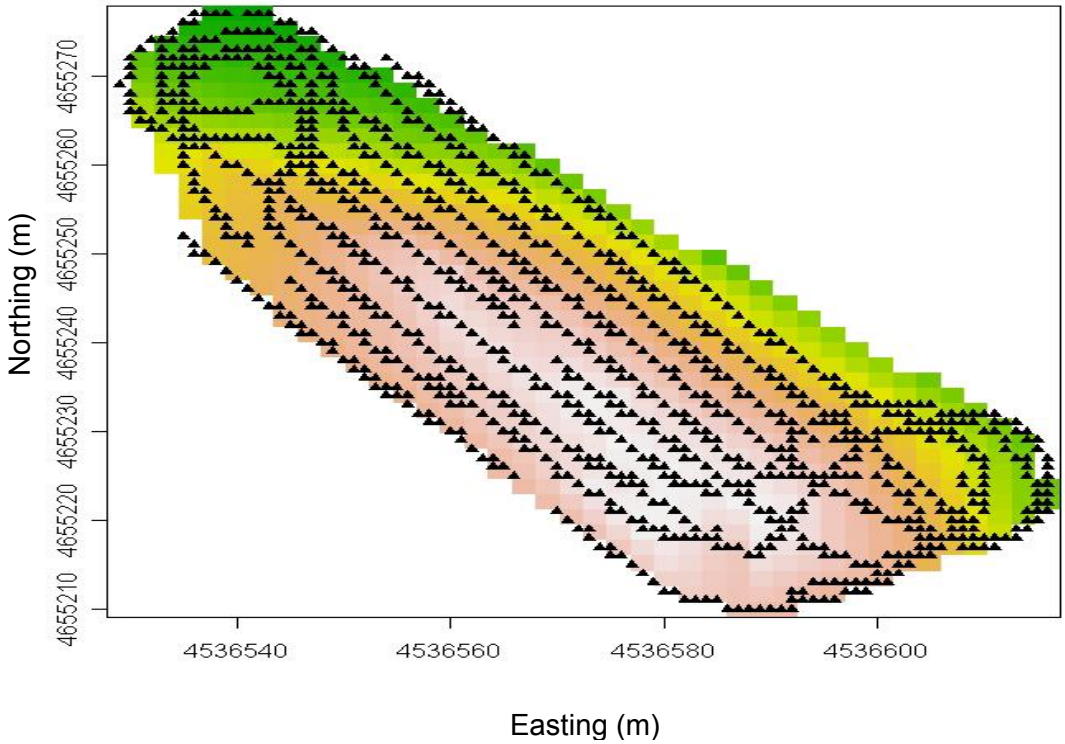

(a)

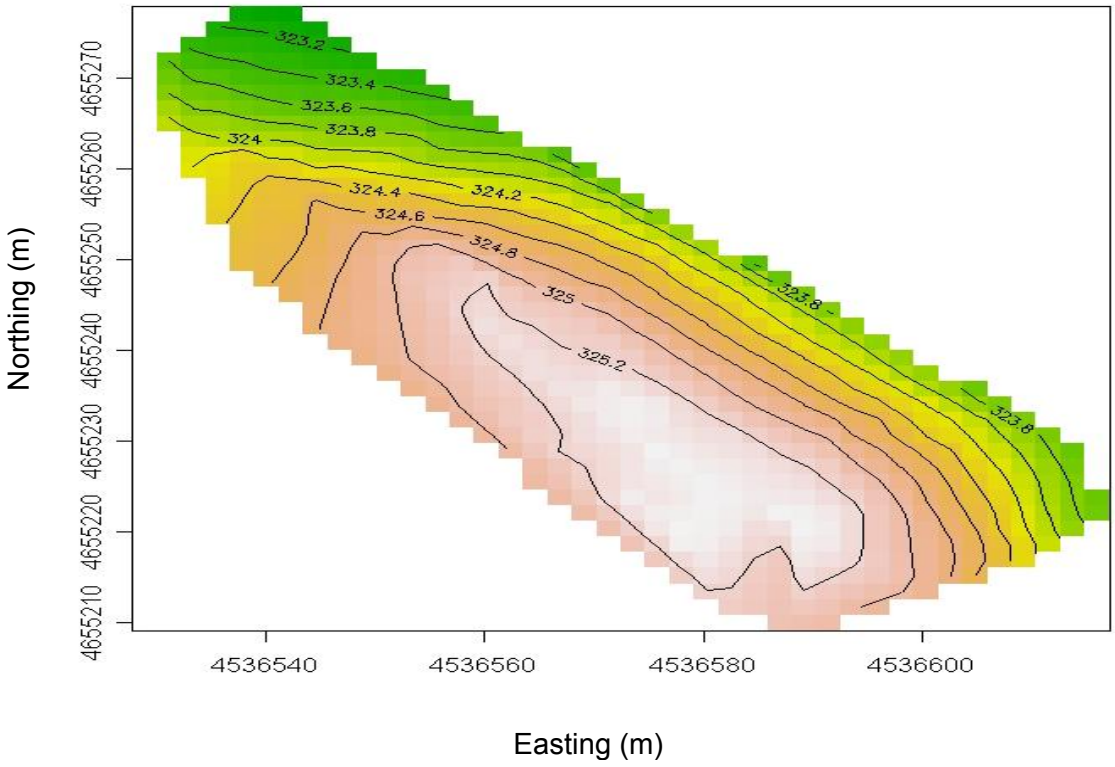

(b)

Figure 1: (a) Vehicle travel path of the Kulvar farm field at low speed test (5.6 km/h)

(b) Topographic map of the same field.

mounted on the sprayer. These pitch angle estimates were noisy as the errors in the RTK-GPS measurements were propagated into the pitch angle calculations.

In sensor fusion process, these error sources need to be taken into account and modeled by an appropriate error modeling technique to improve the performance of the EKF developed for the attitude angle estimation of the sprayer. The next section describes the modeling of the roll angle errors from the TCM sensor and the errors in pitch angle estimates by a single GPS receiver using an autoregressive (*AR*) error modeling technique.

Autoregressive error model

The *AR* modeling was an attempt to standardize the sensor noise so that it can be better described as a white Gaussian noise, an intrinsic assumption of the Kalman filter theory. In many cases when system noise covariance (*Q*) and measurement noise covariance (*R*) were not modeled, they have to be fine tuned for optimal Kalman state estimation (Bergeijk et al., 1998; Kiriy and Buehler, 2002). The fine tuning of both *Q* and *R* is basically a trial-and-error process and can be difficult to employ especially when multiple sensor measurements and multiple state variables have to be incorporated into the Kalman filter design, which is often the case. Though it is difficult to compute the system noise covariance, the measurement noise covariance can be computed, as we acquire the measurements of the system using different onboard sensors. Sensor data could possibly have errors varying from measurement to measurement depending on the sensor characteristics throughout the experiment. In order to account the sensor measurement errors in the fusion process, the *AR* modeling technique was

applied in this research, which in return confers the zero mean white Gaussian noise as a measurement noise covariance *R*.

The determination of an appropriate *AR* model involved a number of interrelated problems such as use of a suitable order selection criterion and estimating the coefficients of the *AR* model. Order selection criteria such as Final Prediction Error (FPE), Akaike Information Criterion (AIC), Bias Corrected AIC i.e. AICC, Schwarz's Information Criterion (SIC), Bayesian Information Criterion (BIC), Minimal Descriptive Length (MDL), PHI Criteria, Haring (HAR) criterion and Jenkins and Watts (JEW) criterion are some of the most commonly used criterions for selecting the order and the coefficients of the sensor noise *AR* modeling (Djuric and Kay ,1993; Babu and Wang, 2004; Broersen, 2005). Liew (2004) found that FPE, AIC, SIC and BIC criteria perform considerably better in estimating the true autoregressive model order for small number of samples. For more understanding of *AR* model order selection criteria see Brockwell and Davis (1996).

FPE criteria selects the *AR* order which minimizes the one-step mean squared error instead of considering the estimated white noise covariance minimization approach like AIC. AIC criterion overestimates the order of the model than FPE for the same given data series (Brockwell and Davis, 1996). Fitting a very high order model generally results in small white noise variance estimation. However, the mean squared error of the forecasted series depends not only on the white noise variance of the fitted model but also on errors arising from the estimation of the parameters of a model (Brockwell and Davis, 1996). Brockwell and Davis (1996) also suggested that for pure autoregressive models Burg's algorithm usually gives higher likelihoods than the Yule-Walker equations. Therefore, in this research, Burg's algorithm was used along with FPE order selection criterion to select the proper *AR* model order and the coefficients. The other AR order selection criteria stated earlier were also used to compute the order of the *AR* model form the slow speed TCM roll measurements. FPE, AIC and all other criteria reported above fitted second order on the modeled roll measurements of the slow speed data, whereas the JEW criterion calculated 5^{th} order on the same data.

These criteria were also used on medium speed TCM roll measurements and a single GPS pitch estimates for slow as well as medium speed datasets to calculate the order of the *AR* model. The estimates showed that the second order is the best choice of the *AR* model order for modeling the slow and medium speed datasets though in most cases JEW criterion estimated higher *AR* order compared to other criteria used in this work. The order obtained from FPE order selection criterion was then used to get *AR* model coefficients which were determined using Burg's method. Kurtosis analysis of the original roll, pitch error and the residual error after AR modeling of the errors was done to observe the standard normal distribution of the errors. Original roll and pitch error distribution had positive Kurtosis-3 value meaning the error distribution was always peaked. The residual error after AR modeling of roll and pitch error had Kurtosis-3 value near zero, meaning the residual error distribution was normal with zero mean (figure 2).

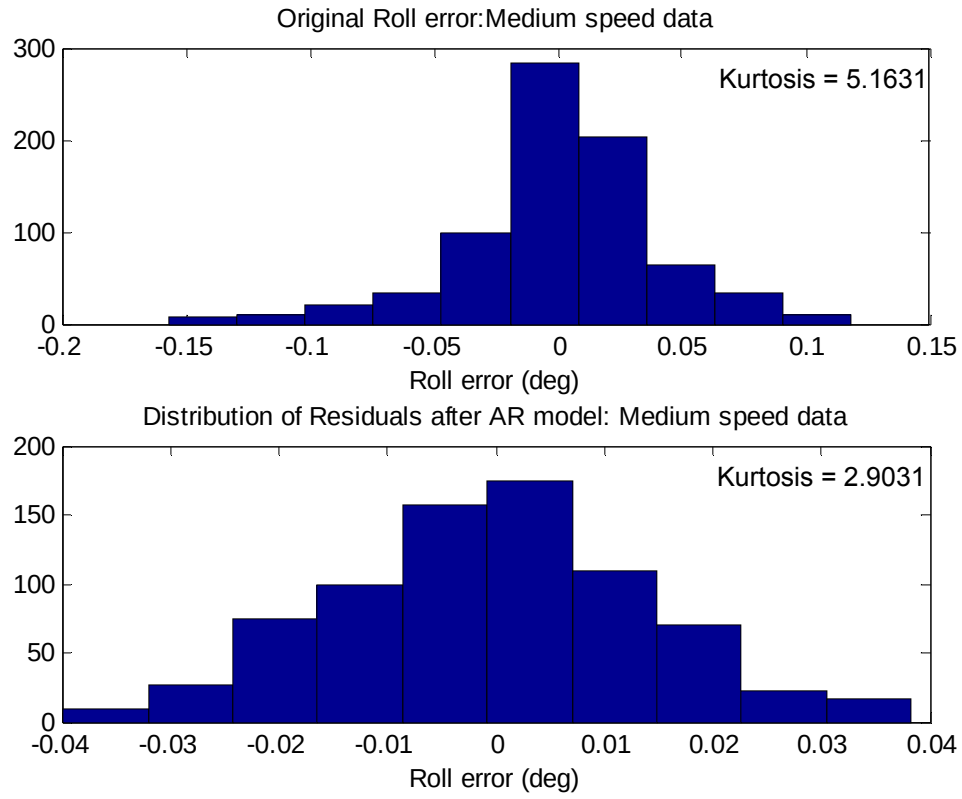

Figure 2: Original TCM roll error and residual error distribution after AR model (Medium speed)

Kalman Filter implementation

The Kalman filter is an extremely effective and versatile procedure for combining noisy sensor outputs to estimate the state of a system with uncertain dynamics (Grewal et al., 2001). An extended Kalman Filter could be used to estimate the nonlinear dynamic system states that can only be observed indirectly or inaccurately by the system itself. State of the system is defined as the minimum information about the past and the present, needed to determine an optimal estimate of the future response using the future noisy measurements (Padulo and Arbib 1974; Wood and Radewan 1977).

Kalman filter estimation of the states improves as the number of processed data points/measurements increases, so to get the quality state vector Wang (1998) used a 2-D kalman filter twice over the same noisy DEM data with different orientations to estimate the terrain variables from the DEM. He found that the above filtering approach reduced the standard deviation of the random noise from the DEMs by 70% for the elevation and 85% for the first partial derivatives of the elevation, compared with their original values. Guo et al. (2003) also developed a low-cost position-velocity-attitude (PVA) model based Kalman filter to provide accurate and robust vehicle positioning data for precision farming applications.

In this research, the EKF algorithm was applied to improve the sprayer attitude angle estimates and also to improve the elevation estimates; the procedure of which is described in the following sub sections. In order to improve the quality of the estimation process, two way Kalman filtering was applied on the same datasets twice; first in the forward direction and second time in reverse

direction; and the average of the estimated states were termed as the estimated states of our interest.

Roll-pitch Kalman filter

The roll and pitch angle estimates of the self-propelled sprayer from DEMs are fused with the roll measurements from the TCM and pitch estimates from the GPS. The system state vector used in this process is defined as:

$$x_k = \left[\phi_k, \theta_k, \phi_{err1_k}, \phi_{err2_k}, \theta_{err1_k}, \theta_{err2_k} \right]^T \quad (1)$$

Where, $ø$, θ are the roll and pitch angles with roll error $ø_{err1}$, $ø_{err2}$, and pitch error θ_{err1}, θ_{err2}.

The above states are represented by the following system function, *f(x)*:

$$f(x) = \left[f_\phi, f_\theta, f_{\phi_{err1}}, f_{\phi_{err2}}, f_{\theta_{err1}}, f_{\theta_{err2}} \right]^T \quad (2)$$

Each system function is characterized by the kinematic equation (Eq. 3 to 8) for the roll and pitch angle estimates of the sprayer along with the error estimates from these angles using EKF algorithm.

$$f_\phi = \phi_{k+1} = \phi_k + \dot{\phi}_k .\Delta T + \varepsilon_\phi \quad (3)$$

$$f_\theta = \theta_{k+1} = \theta_k + \dot{\theta}_k .\Delta T + \varepsilon_\theta \quad (4)$$

$$f_{\phi_{err1}} = \phi_{err1,k+1} = A_{\phi 1}\phi_{err_k} \quad (5)$$

$$f_{\phi_{err2}} = \phi_{err2,k+1} = A_{\phi 2}\phi_{err_{k-1}} \quad (6)$$

$$f_{\theta_{err1}} = \theta_{err1,k+1} = A_{\theta 1}\theta_{err_k} \quad (7)$$

$$f_{\theta_{err2}} = \theta_{err2,k+1} = A_{\theta 2}\theta_{err_{k-1}} \quad (8)$$

where,

k+1, *k* and *k-1* are future, present and previous time steps;

ΔT is sampling interval (s);

$\dot{\phi}$, $\dot{\theta}$ are the roll and pitch rates from the DEM;

$Aø_1$, $Aø_2$, $A_{\theta 1}$, $A_{\theta 2}$ are the *AR* coefficients for the roll and pitch error estimation.

$\varepsilon_ø$, ε_θ are the random white Gaussian noise for roll and pitch.

The first order partial derivatives of the system function (Eq. 2) with respect to system state vector x_k (Eq. 1) are represented as the system Jacobian matrix, A_k

$$A_k = \begin{pmatrix} 1 & 0 & 0 & 0 & 0 & 0 \\ 0 & 1 & 0 & 0 & 0 & 0 \\ 0 & 0 & A_{\phi 1} & 0 & 0 & 0 \\ 0 & 0 & 0 & A_{\phi 2} & 0 & 0 \\ 0 & 0 & 0 & 0 & A_{\theta 1} & 0 \\ 0 & 0 & 0 & 0 & 0 & A_{\theta 2} \end{pmatrix}_{x_k} \quad (9)$$

The DEM estimated roll, pitch rates used in system kinematic equations (Eq. 3 and 4) are taken as the control inputs $u_k = \begin{bmatrix} \dot{\phi} & \dot{\theta} \end{bmatrix}^T$. The input Jacobian matrix (B_k) is then derived by taking partial derivatives of system function *f(x)* (Eq. 2) with respect to these inputs:

$$B_k = \begin{pmatrix} \Delta T & 0 \\ 0 & \Delta T \\ 0 & 0 \\ 0 & 0 \\ 0 & 0 \\ 0 & 0 \end{pmatrix}_{x_k} \quad (10)$$

The measurement vector (Eq. 11) consisted of the roll angle measurements from the TCM sensor and the pitch angles derived from a single GPS antenna mounted on the sprayer. The roll and pitch angle errors from these measurements were modeled using the *AR* modeling technique as discussed in the previous section. Errors as estimated by the EKF error states were then subtracted from the measurements before using these measurements to calculate the EKF estimates of the roll and pitch angles.

$$z_k = \begin{bmatrix} \phi_{TCM} - \phi_{err1_k} - \phi_{err2_k}, \theta_{GPS} - \theta_{err1_k} - \theta_{err2_k} \end{bmatrix}^T \quad (11)$$

The measurement Jacobian matrix (H_k) which relates the measurements (Eq. 11) with the system states of our interest (Eq. 1) is derived as below:

$$H_k = \begin{pmatrix} 1 & 0 & -1 & -1 & 0 & 0 \\ 0 & 1 & 0 & 0 & -1 & -1 \end{pmatrix}_k \quad (12)$$

Easting-Northing-Up (ENU) Kalman filter

Though the prime objective of this research was to improve the attitude angles of the sprayer estimated by the DEMs and other complementary sensors using the sensor fusing technique, it was necessary to examine how the improved attitude affects on the elevation measurements of the GPS used to formulate DEMs and also on orientation of the sprayer. EKF state vector (Eq. 13) used for this purpose consisted of the self-propelled sprayer position in Easting (P_E), Northing (P_N), Up (P_U) directions and the sprayer heading (ψ) as the filter estimation parameters.

$$x_k = \begin{bmatrix} P_{E,k}, P_{N,k}, P_{U,k}, \psi_k \end{bmatrix}^T \quad (13)$$

The above states are represented by following system function, *f(x)*:

$$f(x) = \left[f(P_E), f(P_N), f(P_U), f(\psi) \right]^T \quad (14)$$

Roll, pitch and yaw (RPY) angles specified the attitude of the sprayer in the vehicle coordinates i.e. RPY coordinates. The coordinate transformation matrix from RPY to East-North-Up (*ENU*) coordinates is as given below:

$$C_{ENU}^{RPY} = \begin{pmatrix} \sin\psi\cos\theta & \cos\phi\cos\psi + \sin\phi\sin\psi\sin\theta & -\sin\phi\cos\psi + \cos\phi\sin\psi\sin\theta \\ \cos\psi\cos\theta & -\cos\phi\sin\psi + \sin\phi\cos\psi\sin\theta & \sin\phi\sin\psi + \cos\phi\cos\psi\sin\theta \\ \sin\theta & -\sin\phi\cos\theta & -\cos\phi\cos\theta \end{pmatrix} \quad (15)$$

The kinematic equations (Eq. 16 to 19) governing Easting, Northing, elevation and heading states of the sprayer (Eq. 13) were formulated using the above transformation matrix and represented in the system function (Eq. 14).

$$f(P_E) = P_{E,k+1} = P_{E,k} + C_{ENU11}^{RPY}.v_x.\Delta T + C_{ENU21}^{RPY}.v_y.\Delta T + C_{ENU31}^{RPY}.v_z.\Delta T + \varepsilon_E \quad (16)$$

$$f(P_N) = P_{N,k+1} = P_{N,k} + C_{ENU12}^{RPY}.v_x.\Delta T + C_{ENU22}^{RPY}.v_y.\Delta T + C_{ENU32}^{RPY}.v_z.\Delta T + \varepsilon_N \quad (17)$$

$$f(P_U) = P_{U,k+1} = P_{U,k} + C_{ENU13}^{RPY}.v_x.\Delta T + C_{ENU23}^{RPY}.v_y.\Delta T + C_{ENU33}^{RPY}.v_z.\Delta T + \varepsilon_U \quad (18)$$

$$f(\psi) = \psi_{k+1} = \psi_k + \dot{\psi}_k \Delta T + \varepsilon_\psi \quad (19)$$

In equations (16-19) v_x, v_y *and* v_z are the self-propelled sprayer travel velocities in x, y and z direction, respectively and $\dot{\psi}$ is the yaw rate from the TCM sensor. Sprayer travel velocities, yaw rate, roll and pitch angle estimated by the roll-pitch *EKF* filter were taken as the inputs in this filter implementation.

The GPS measurements were used in the measurement vector (Eq. 20), and were compared with prior states estimated by EKF to enhance the overall state estimation during the filtering process.

$$z_k = \left[P_{E,gps},\ P_{N,gps},\ P_{U,gps},\ \psi_{gps} \right]_k^T \quad (20)$$

where, $P_{E,gps}$, $P_{N,gps}$ $P_{U,gps}$ and ψ_{gps} are Easting, Northing, Up and heading measurements of the sprayer from GPS receiver, respectively. The state, input and measurement Jacobian matrices were developed using the same process used for roll-pitch kalman filter as explained in the previous section.

Results and Discussion

The roll-pitch Kalman filter was implemented on the data collected at two speed levels, 5.6 km/h and 9.6 km/h, of the self-propelled sprayer. For each speed level, the DEM of the field was generated using RTK-GPS data. The latitude and longitude measurements from the RTK-GPS receiver were converted to the UTM coordinates. These UTM coordinates and the heading angle measurements from the GPS were then used to obtain the UTM coordinate positions of each of the four wheels of the self-propelled sprayer. The four wheel positions and the elevation of each wheel obtained from the DEM along with other static vehicle measurements were used to obtain the roll and pitch angles of the self-propelled sprayer. The DEM estimated roll and

pitch angles were then fused with the TCM sensor roll data and the pitch estimates from a single GPS receiver. The second order *AR* model was used to model the roll measurements from the TCM sensor and also to model the pitch estimated from the GPS measurements. Table 3.1 shows the autoregressive model coefficients obtained for the second order *AR* model using burg's method.

Table 3.1 Autoregressive model coefficients for roll and pitch angle using 2nd order *AR* model

Sprayer Path	Coefficients for Roll		Coefficients for Pitch		Residual (degree)	
	$A_{ø1}$	$A_{ø2}$	$A_{θ1}$	$A_{θ2}$	*Error* $_{ø}$	*Error* $_{θ}$
Low Speed	0.5874	0.3441	0.6575	0.2748	1.08E-04	4.87E-05
Medium Speed	0.6930	0.2260	0.7285	0.1415	3.01E-04	1.25E-04
Average	**0.6402**	**0.2851**	**0.6930**	**0.2081**	**2.04E-04**	**8.68E-05**

These coefficients were used to estimate the error from the roll and pitch angle measurements so that the white Gaussian noise, residue of the noise, should be separated from the other sources of errors in the angle measurements. Residual error obtained by the *AR* modeling technique could be used as a measurement noise covariance (*R*) in the Kalman filter implementation. Roll and pitch angles along with the roll, pitch errors were considered as the system states in the EKF implementation. Equation 21 is the system noise covariance matrix used in roll-pitch Kalman filter implementation. Residual of the roll and pitch angle error obtained using *AR* error modeling technique (Table 3.1) was used as a measurement noise covariance matrix as shown in equation 22. Fine tuning of the system noise covariance matrix (*Q*) and the measurement noise covariance matrix (*R*) is a key process in improving the performance of an optimal, recursive EKF algorithm. In this research, fine tuning of the EKF *Q* matrix was straightforward as the *R* matrix values were already determined by the *AR* error modeling. System noise covariance *Q* was calculated for different angle error values and it was observed that the performance of the EKF was better at the angle error of 0.11º i.e. at the error covariance value of $(\sigma_{DEM})^2 = 3.68e^{-6}$.

The system noise covariance matrix, *Q*:

$$Q = \begin{pmatrix} 3.68\times10^{-6} & 0 & 0 & 0 & 0 & 0 \\ 0 & 3.68\times10^{-6} & 0 & 0 & 0 & 0 \\ 0 & 0 & 3.68\times10^{-6} & 0 & 0 & 0 \\ 0 & 0 & 0 & 3.68\times10^{-6} & 0 & 0 \\ 0 & 0 & 0 & 0 & 3.68\times10^{-6} & 0 \\ 0 & 0 & 0 & 0 & 0 & 3.68\times10^{-6} \end{pmatrix} \quad (21)$$

The measurement noise covariance matrix, *R*:

$$R = \begin{pmatrix} 2.04\times10^{-4} & 0 \\ 0 & 8.68\times10^{-5} \end{pmatrix} \quad (22)$$

The noise covariance for the roll and pitch angle rates, which were used as a input during the state estimation process, from DEM estimates were fine tuned from 0.1º/sec to 0.05º/sec for improved EKF estimation process. Thus, the roll and pitch rate input noise covariance was taken as $(\sigma_{ø})^2 = (\sigma_{\theta})^2 = (0.05º/sec)^2 = 7.62e^{-7}$ (radian/sec)^2. The input noise covariance matrix, Γ was:

$$\Gamma = \begin{pmatrix} 7.62\times10^{-7} & 0 \\ 0 & 7.62\times10^{-7} \end{pmatrix} \tag{23}$$

Roll and pitch angle estimates of the self-propelled sprayer using DEMs were very noise. Sometimes attitude angle estimates of the sprayer from the DEMs were not continuous as the sprayer path was out of bound from the generated DEMs. The results obtained from the developed EKF algorithm on slow speed data for the roll and pitch angle estimation are as shown in figure 3 and 4. The IMU measurements of the roll and pitch angles were used as a reference during the EKF implementation to validate the effectiveness of the developed algorithm. For roll and pitch angle estimates of the sprayer from DEMs, the straight line on the DEM roll and pitch plot with zero as a measurement (fig. 3.3, 3.4) shows that the sprayer was out of bound from generated DEM of the field. Out of bound circumstances did not provide the roll and pitch angle estimates from the DEM and therefore, the EKF algorithm has to rely on the TCM roll measurements and a single GPS-based pitch estimates to improve the attitude angles of the sprayer during the EKF estimation process. EKF algorithm was effective in estimating the attitude angles in the out of bound circumstances which can be seen in figure 2 and 3. EKF estimated roll and pitch angles were close to the IMU measurements though the DEMs estimates were absent or away from the IMU measurements. TCM roll angle measurements (fig. 3) and a single GPS-based pitch angle estimates (fig. 3) were close to the reference IMU measurements but had high-frequency noise associated with them. The implemented EKF algorithm was successful in removing the noise from these sources which is evident in figure 3 and 4, respectively. Table 2 summarizes the mean as well as the standard deviation of the roll and pitch angle errors obtained for the slow and medium speed tests.

The roll and pitch angle errors from different sensor sources were obtained by considering the IMU measurements as standard reference measurements. For the slow and medium speed data, the standard deviation of the roll error from the EKF estimates was less as compared to the roll errors from TCM as well as DEM roll angle estimates.

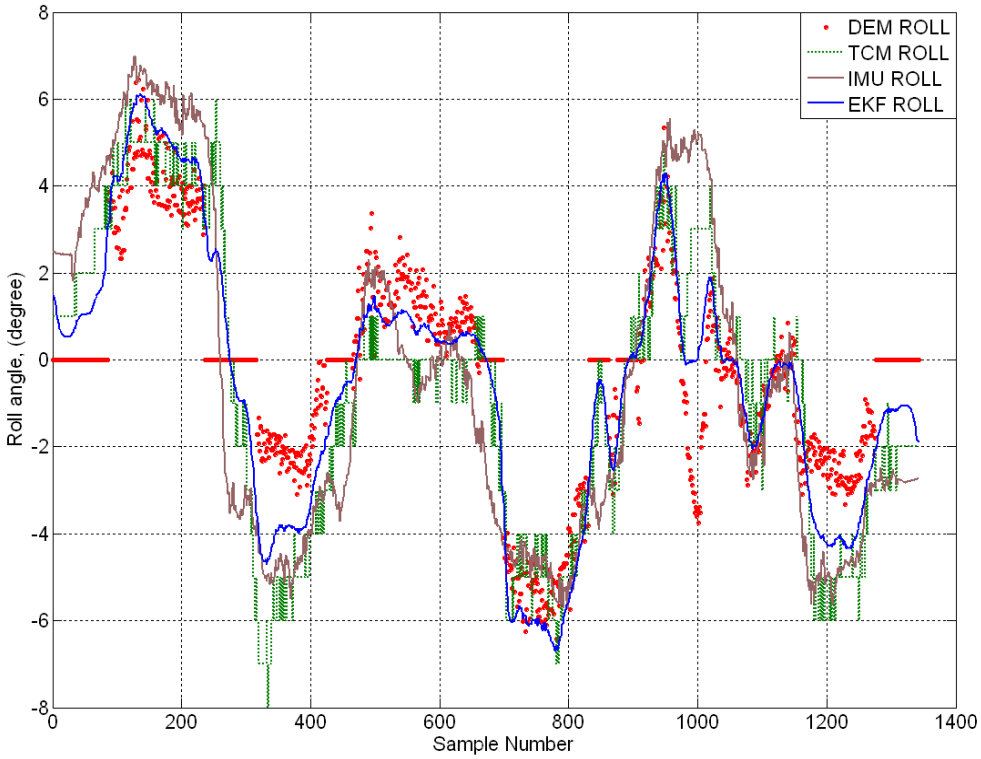

Figure 3: Roll angle from DEM, TCM, IMU and EKF for slow speed of the sprayer vehicle.

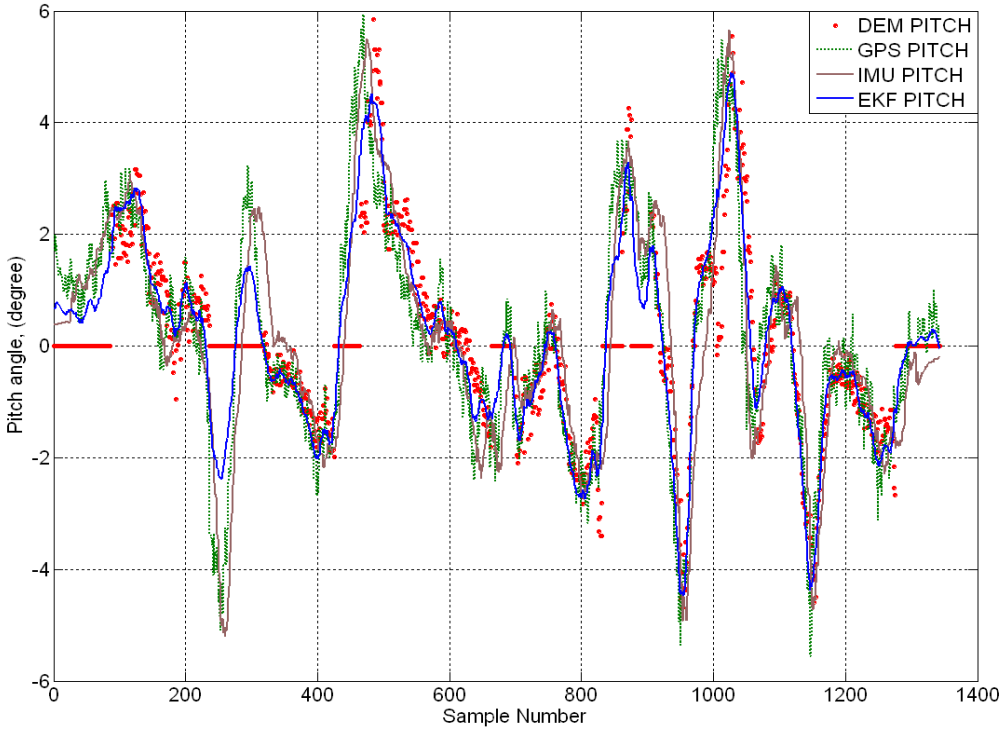

Figure 4: Pitch angle from DEM, TCM, IMU and EKF for slow speed of the sprayer vehicle.

Table 2: Roll and pitch error from different sources compared to EKF with IMU as a reference.

Sprayer Path		Roll Error		Pitch Error	
		Mean	Std. Dev.	Mean	Std. Dev.
Slow Speed	DEM	0.2157	2.4610	-0.0473	1..3230
	TCM Roll	-0.2320	1.4220		
	GPS Pitch			0.0473	0..9848
	EKF	**-0.2244**	**1.4710**	**0.0597**	**0.6621**
Medium Speed	DEM	0.0912	2.4500	0.0131	1.7620
	TCM Roll	-0.0725	2.2860		
	GPS Pitch			-0.0131	1.2220
	EKF	**-0.0430**	**2.5490**	**0.0140**	**0.9145**

Standard deviation of the pitch error from the EKF estimates were considerably lower, except the standard deviation of EKF estimated pitch for medium speed dataset, when compared to the pitch error from the DEMs as well as the pitch angle error from GPS-based pitch for both the speed levels. For medium speed pitch estimates using EKF, though the standard deviation was higher, the EKF considerable reduced the high frequency error associated with GPS-based pitch estimates and the estimates were smoother and continuous when compared to that of DEM estimated pitch.

The improved attitude angles using roll-pitch EKF algorithm were then used to estimate the three dimension (3D) position of the self-propelled sprayer. The preciseness of the elevation measurements is important in creating the highly accurate DEMs of the topographic field as well as in the attitude angle estimates using DEMs. The GPS receiver mounted on the self-propelled sprayer had height of about 3.81 m from the ground when the sprayer is on flat surface. Figure 5 shows the effect of the vehicle role on GPS elevation and position measurements. Similar effect of pitch and yaw angle offset affects the GPS measurements. The roll, pitch and yaw angle of the vehicle at a given timestep affects the measured position of the vehicle and this position need to be corrected by removing the attitude angle effects. Equation 24 shows the rotation matrices due to the roll-pitch-yaw {(Rx, ϕ), (Ry, θ), (Rz, ψ)} of the vehicle about the x, y and z in the vehicle coordinate system, respectively. To analyze the error bounds and the potential improvements in position and elevation estimates, the following analytical process was conducted. If we assume that the original vehicle position in the vehicle coordinate at point P^T_{xyz} is $\begin{bmatrix}0 & 0 & 3.81\end{bmatrix}$, the roll-pitch-yaw corrected vehicle position P'_{xyz} will be calculated using eq.25.

$$(Rx, \phi) = \begin{pmatrix} 1 & 0 & 0 \\ 0 & \cos\phi & -\sin\phi \\ 0 & \sin\phi & \cos\phi \end{pmatrix} \qquad (Ry, \theta) = \begin{pmatrix} \cos\theta & 0 & \sin\theta \\ 0 & 1 & 0 \\ -\sin\theta & 0 & \cos\theta \end{pmatrix}$$

$$(Rz, \psi) = \begin{pmatrix} \cos\psi & -\sin\psi & 0 \\ \sin\psi & \cos\psi & 0 \\ 0 & 0 & 1 \end{pmatrix} \qquad (24)$$

$$P'_{xyz} = (R_x, \phi) \times (R_y, \theta) \times (R_z, \psi) \times P^T_{xyz} \qquad (25)$$

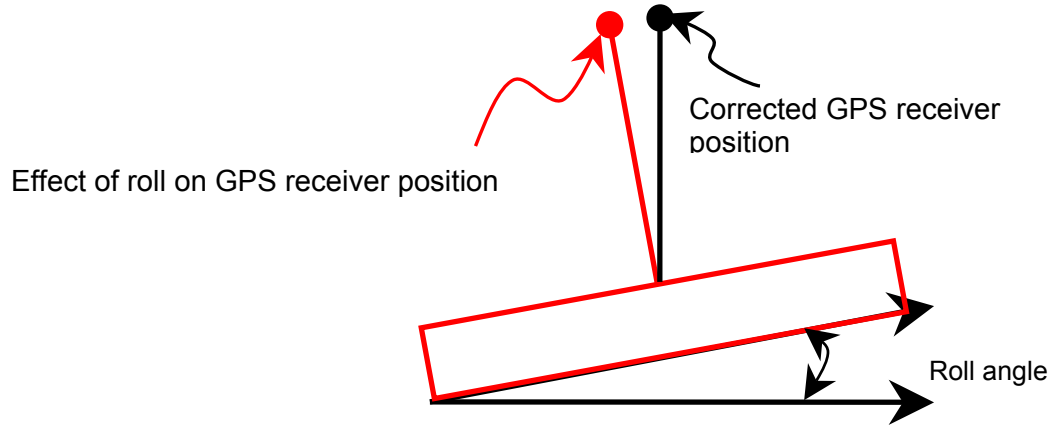

Figure 5: Effect of roll angle experienced by sprayer on GPS measurements.

The roll and pitch error reported in table 2 with IMU as a reference has maximum std. dev. error of 2.46º for roll and maximum std. dev. error of 1.32º for pitch from the DEMs. For these roll and pitch errors, the analytical computation confirmed that the expected elevation error will be about 0.53 cm where as the error in x and y positioning of the sprayer will be about 11.71 cm and 16.34 cm, respectively. In worst case scenario, the maximum roll angle error from DEMs was about 8.95º and the maximum pitch angle error from the DEMs was about 5.45º. The worst case attitude angle errors were also used to calculate the expected position and elevation error of the self-propelled sprayer. The analytical calculation for these attitude errors showed that the expected elevation error will be about 6.33 cm in the worst case scenario. The RTK-GPS elevation measurements also suffer from the regular inconsistencies in the elevation due to the Dilution of Position (DOP) variation during the experimental runs. These attitude and other errors need to be accounted for while improving the elevation from the GPS sensor measurements. EKF algorithm implemented for improving the sprayer positioning estimates and most importantly the GPS elevation measurements showed promising results. Figure 6 shows the RTK-GPS elevation measurements and the EKF estimated elevations on the slow speed datasets. Figure 7 shows the 3D travel trajectory of the self-propelled sprayer as measured by the GPS and estimated by the proposed EKF algorithm. The implemented EKF algorithm showed promising results in improving the elevation measurements for slow and medium speed data. The GPS measured trajectory was noisy and had sudden jumps in elevation measurements (fig 7). EKF algorithm was able to estimate smoother trajectory compared to that of GPS measured trajectory and was also successful in removing the sudden jumps in measurements which were due to the variation in DOP during experimental runs. The error range in elevation from the GPS measurements was from 0.53 cm to 6.33 cm for the given datasets as calculated during analytical work. However, due to the absence of the *AR* model for GPS data, the fine tuning of the system (*Q*) and measurement (*R*) matrices was critical in the EKF implementation.

In DEMs development using the vehicle based measurements, the accuracy of the DEMs creation depends not only on the accurate elevation measurements but also on the number of the vehicle field passes (Clark and Lee 1998). The DEMs development and enhancement is out-of-scope of this research, however, it can be suggested that the EKF improved vehicle elevation estimates could be useful in creating DEMs with better accuracy via any DEMs development algorithm and also to estimate the accurate vehicle attitude angles when the vehicle is traveling in the field, of which the DEM is available in advance.

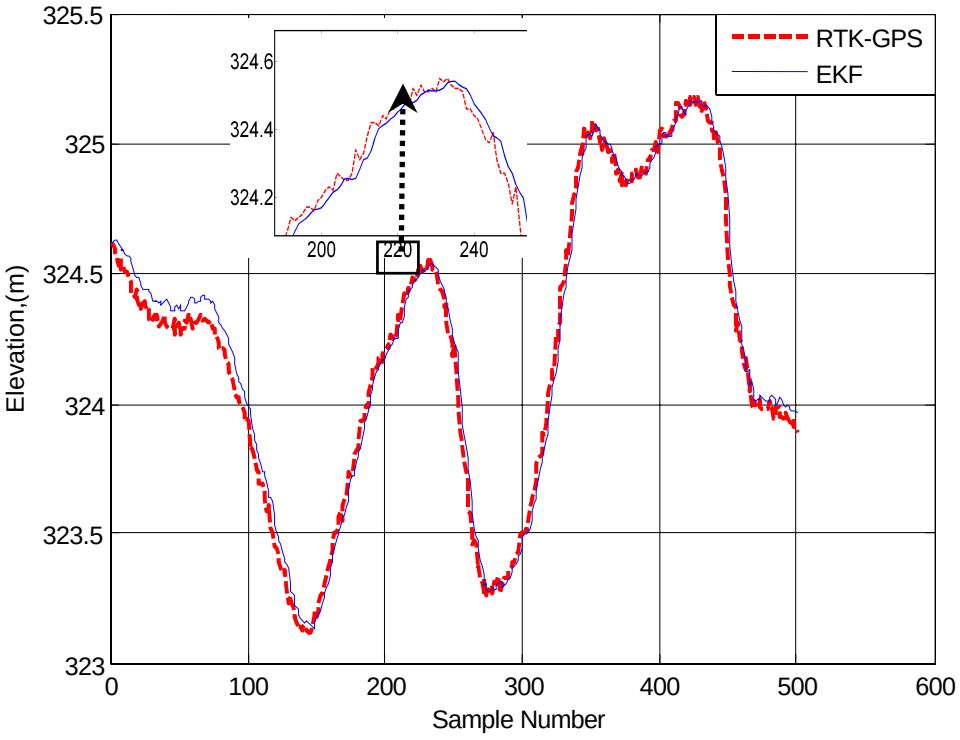

Figure 6: RTK-GPS elevation measurements and EKF estimates using sprayer attitude angles.

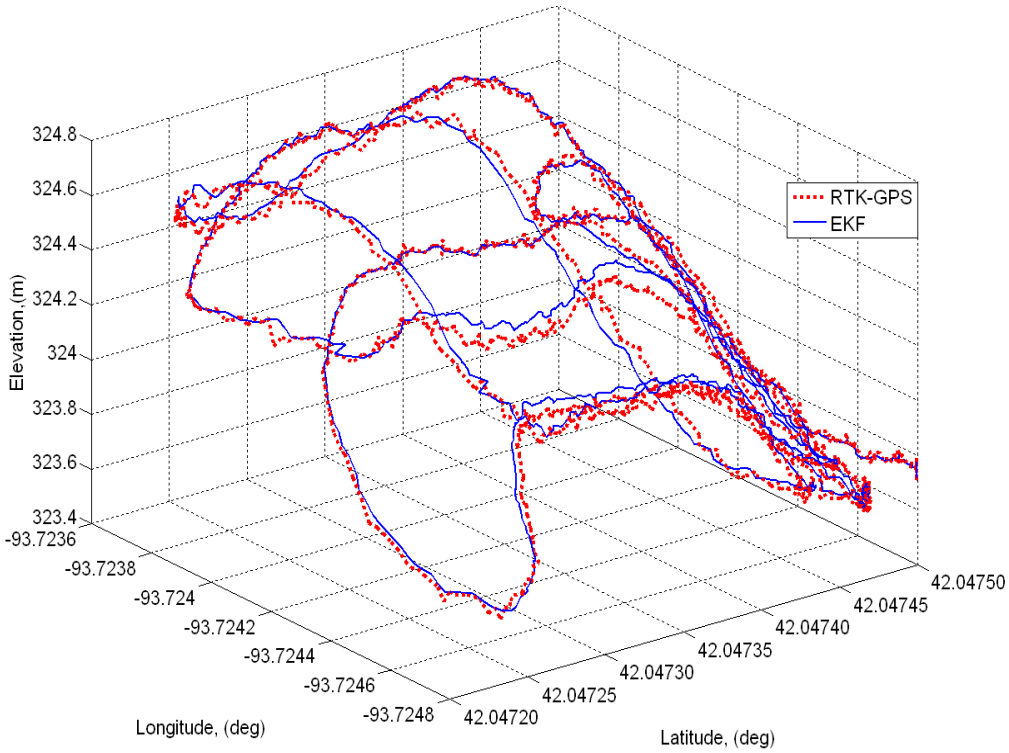

Figure 7: Sprayer travel trajectory (3D) measured by RTK-GPS and estimated by EKF data fusion technique.

Conclusion

From this research following conclusions can be drawn:

- The developed roll-pitch EKF algorithms was effective in improving the attitude angle estimates of the self-propelled sprayer by fusing the DEMs roll and pitch estimates with the TCM roll measurements and a single GPS-based pitch estimates, respectively.
- The EKF algorithm was effective in estimating the sprayer attitude angles even when the DEMs attitude estimates were not available for certain period due to the out of bound circumstances of the DEMs. The EKF algorithm was also capable of removing the high frequency noise associated with the TCM and GPS sensor measurements.
- The accurate elevation measurements are important in developing the highly accurate DEMs. The Kalman filtering technique improved the elevation accuracy of the GPS sensor measurements for sprayer path datasets at both the speed levels by removing the elevation offset due to the roll and pitch angle errors.
- The AR modeling of the attitude angle measurements for the sprayer paths improved the quality of roll-pitch EKF implementation and reduced the manual fine tuning efforts. This research could be useful in more accurately estimating the attitude angles of the vehicle traveling in the field of which the topographic map is available in advance, without the use of IMU, TCM and other attitude angle measurement sensors. This research might also be helpful in creating DEMs with more accurate elevation estimates.

References

Babu, R., and J. Wang. 2004. Improving the quality of IMU-derived Doppler estimates for ultra-tight GPS/INS integration. GNSS2004 Paper 144, Rotterdam, Netherlands. Available at http://www.gmat.unsw.edu.au/snap/publications/. Accessed 10 May 2005.

Bergeijk, V. J., D. Goense, K.J. Keesman, and L. Speelman. 1998. Digital filters to integrate Global Positioning System and dead reckoning. *J. Agric. Eng. Res.* 70(2):135-143.

Bolstad, P.V. and T. Stowe. 1994. An Evaluation of DEM accuracy: Elevation, slope, and Aspect. *Photogrammetric Engineering and Remote Sensing*, 60(11): 1327-1332.

Brockwell, P. J. and R.A. Davis. 1996. *Introduction to time series and forecasting*, Springer-Verlag New York Inc. New York.

Clark, R. L., and R. Lee. 1998. Development of topographic maps for precision farming with kinematic GPS. *Transactions of the ASAE* 41(4): 909-916.

Colvocoresses, A. P. 1993. GPS and the topographic map. *Photogram. Eng. & Remote Sens.* 59(11): 1593-1594.

Deere. 2003. Accurate positioning with the StarFire network guiding a tractor over rough terrain. *Breaking ground*. Fall/winter 2003. Urbandale, Iowa: John Deere Ag Management Solutions.

Djuric, P. M. and S. M. kay. 1993. Order selection of autoregressive models. *IEEE Transactions on Signal Processing*, 40 (11): 2829-2833.

Grewal M. S., L. R. Weill and A. P. Andrews. 2001. *Global positioning systems, inertial navigation and integration*. New York, A John Wiley & Sons, Inc. Publication

Guo L. S., Q. Zhang, and L. Feng. 2003. A low-cost integrated positioning system of GPS and inertial sensors for autonomous agricultural vehicles. P*resentation paper at the 2003 ASAE Annual international meeting*, Las Vegas, NA. Paper Number: 033112.

Kiriy, E., and M. Buehler. 2002. Three-state extended Kalman filter for mobile robot localization. Tech. Report Centre for Intelligent Machines (CIM), McGill University, Canada. Available at http://www.cim.mcgill.ca/. Accessed 25 March 2005.

Liew, V. K. 2004. On autoregressive order selection criteria. *Computational Economics,* Paper no. 0404001, Economics Working Paper Archive EconWPA.

Padulo, P. and M. A. Arbib. 1974. *System Theory: A unified state-space approach to continuous and discrete systems*, Muze Inc., Philadelphia

Wang, P. 1998. Applying two dimensional kalman filtering for digital terrain modeling. *IAPRS: GIS between vision and applications* 34(4): 649-656

Westphalen, M. L., B. L. Steward and S. Han. 2004. Topographic mapping through measurement of vehicle attitude and elevation. *Transactions of the ASAE* 47(5): 1841-1849.

Woods, J.W. and C. H. Radewan. 1977. Kalman filtering in two dimensions. *IEEE Transactions on Information Theory*, IT-23(4): 473-482.

Yao, H. and R. L. Clark. 2000. Development of topographic maps for precision farming with medium accuracy GPS receivers. *Transactions of the ASAE*, 16(6): 629-636.